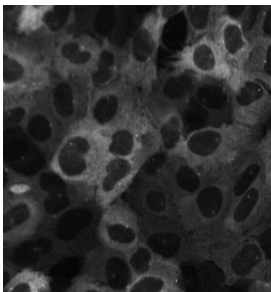
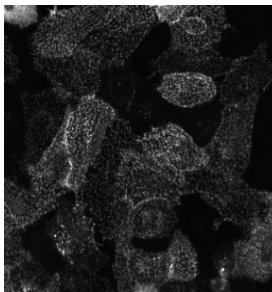
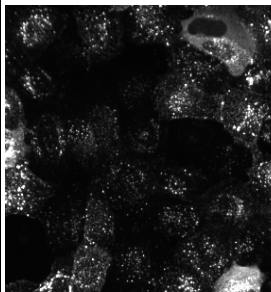
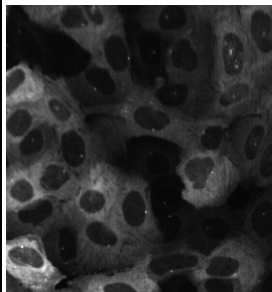
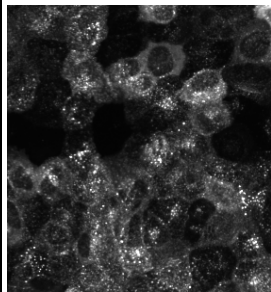
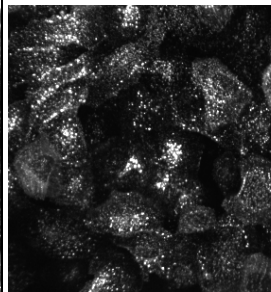
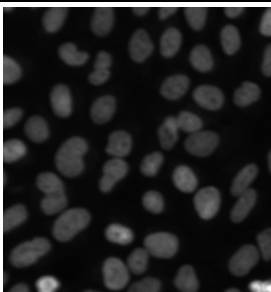
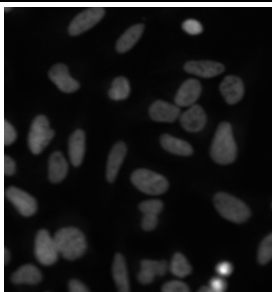
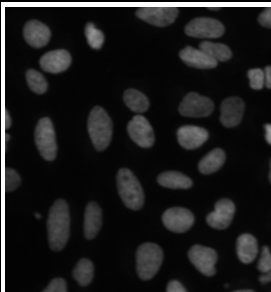
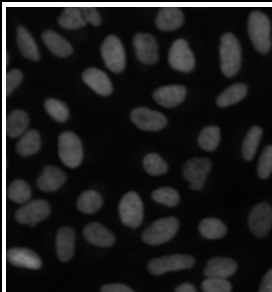
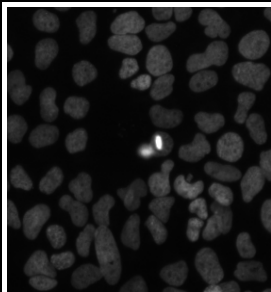
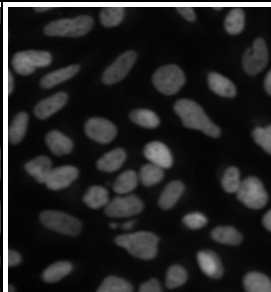
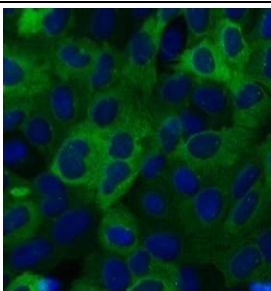
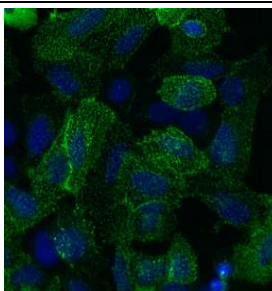
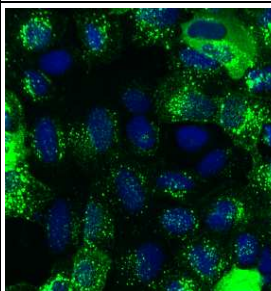
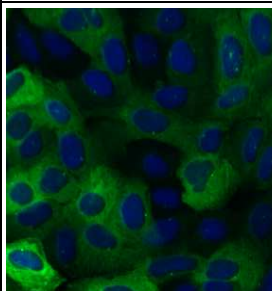
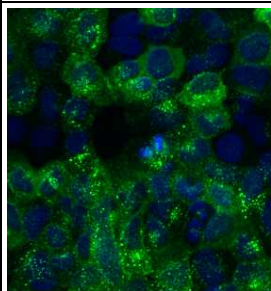
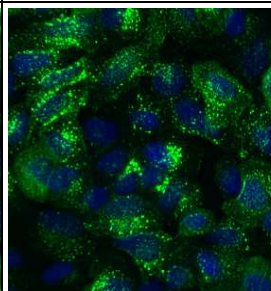
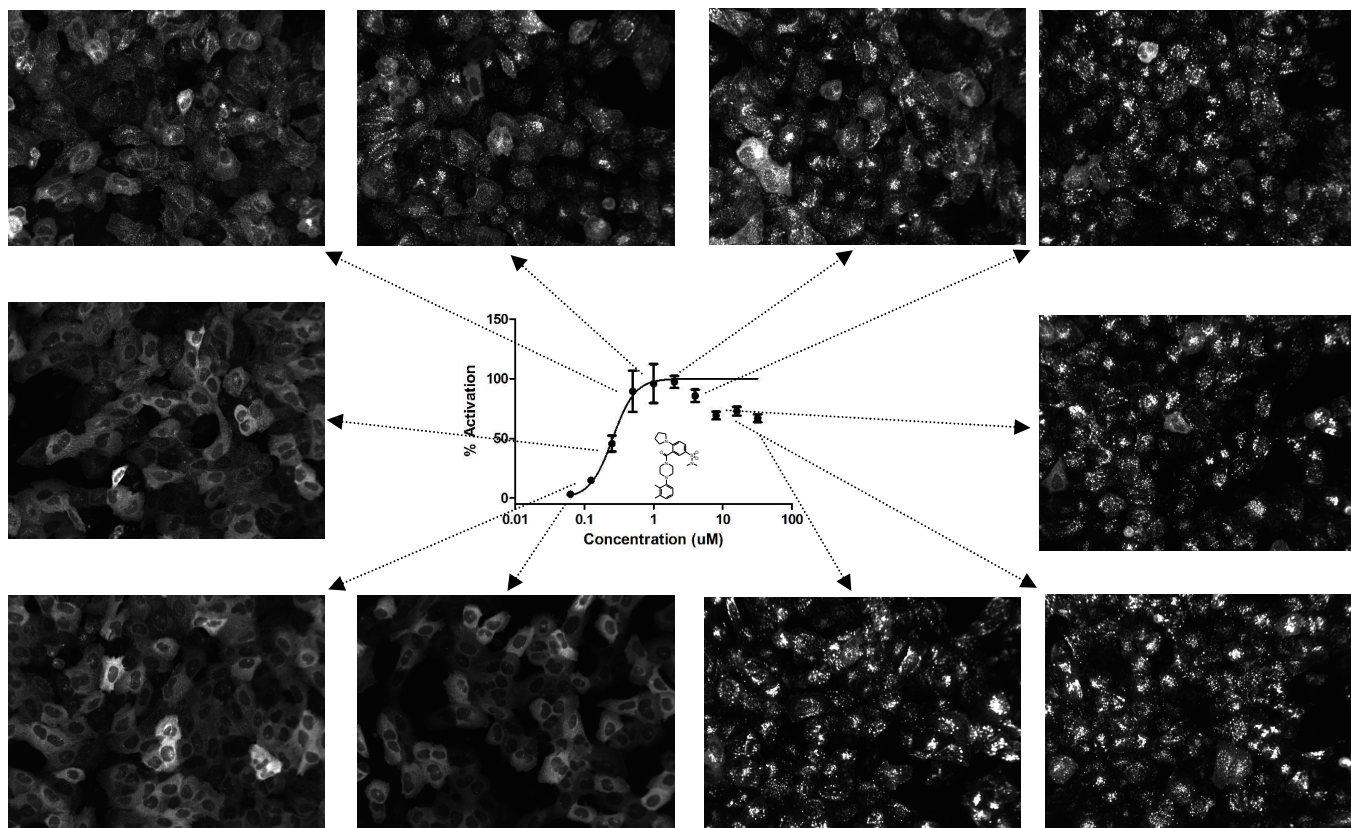


SUPPLEMENTAL INFORMATION

Table S-1. Example Images from $\beta$ -Arrestin Assay						
	Negative Control DMSO	Positive Control [10uM LPI]	1792197 [1uM]	1135734 [1uM]	1172084 [1uM]	2440433 [1uM]
GFP- Labeled $\beta$ -Arrestin						
Dapi-Stained Nuclei						
Pseudo-Colored Overlay						



**Figure S-1 Functional Read-Out**

The dose response curves in Figure 3A in the text reach 100% activation as compared to LPI and then drop back down to a slightly lower plateau. This is likely due to a combination of the biology of the pit/vesicle formation with the image analysis assay read-out. The primary assay read-out is based on the well average of the “Number of Spots Detected per Cell” parameter. As higher concentrations of the compounds are added, the pits either cannot be resolved properly and multiple pits may be detected as one larger pit or the pits merge into larger vesicles, resulting in an apparent drop of activity at higher concentrations. It is best to zoom in to >250% to see the smaller dimmer spots well. In addition, it is possible that solubility problems at higher concentrations may also be contributing to this drop to a lower plateau.

### **Details of the Selected TMHs Incorporated in the R and R\* models.**

The TMH1 conformer chosen for incorporation in our model had a bend angle of 21.1°, a wobble angle of 163.7°, and a face shift of 43.2° (values calculated in ProKink using P1.41 as the hinge residue).

The TMH2 conformer chosen for our model had a bend angle of 28.4°, a wobble angle of -100.1°, and a face shift of 67.3° (hinge residue: P2.58).

The incorporated TMH5 helix had a bend angle of 14.6°, a wobble angle of -160.6°, and a face shift of 20.9° (hinge residue: P5.41).

The TMH6 conformer chosen for the inactive bundle has a bend angle of 32.2°, a wobble angle of -97.8°, and a face shift of 54.0° whereas the TMH6 conformer chosen for the active bundle has a bend angle of 25.7°, a wobble angle of -98.3°, and a face shift of 68.4°)

When the  $\chi_1$  of F6.48(239) is in g-plus (inactive state conformation), the  $\chi_1$  of H6.52(243) prefers the g-plus position. When the  $\chi_1$  of F6.48(239) is trans (activated state), the  $\chi_1$  of H6.52(243) prefers trans. The TMH6 chosen for the GPR55 R\* state has the  $\chi_1$  of both F6.48(239) and H6.52(243) in trans.

The TMH7 chosen for the initial GPR55 model had a bend angle of 12.0°, a wobble angle of 162.8°, and a face shift of 0.2° (hinge residue: V7.50), however, during the energy minimization,

TMH7 developed a larger bend angle due to N7.43 interacting with the backbone of TMH7 (bend angle= 31.9°, wobble angle= 173.0°, face shift= -0.9°). The proximity of methionines on TMH7 (M7.39) and TMH2 (M2.61) caused the EC end of TMH7 to bend away from the bundle as TMH2 and TMH7 packed during the minimization.

**Table S-2. The correlation of  $\chi_1$  of F6.48 (239) with F6.44 (235) and H6.52 (243).**

$\chi_1$ of serine 6.47 (238) was held in trans position							
		F 6.44		H 6.52		Bend angle	Wobble angle
		g plus	trans	g plus	trans		
F 6.48	g plus	30.%	70.%	81.%	19.%	*40.5 ± 16.3	*-56.7 ± 60.5
	trans	4.%	96.%	3.%	97.%	*29.9 ± 7.6	*-101.7 ± 74.7

\*Values are presented as mean ± SD.

### Minimum Energy Conformers of GPR55 Agonists (2-4) and Control Compound (5).

The global minimum energy conformer of CID1792197 (**2**) has the section of the molecule linking ring B and the *ortho*-methoxy ring almost planar ( $C4''-N3-C4-N5 = -176.6^\circ$ ,  $N3-C4-N5-C6 = 4.2^\circ$  and  $N5-C6-C8-C9 = 180.0^\circ$ ) with the N3 of the thiourea hydrogen bonding to the carbonyl oxygen O7 (N-O distance is 2.69Å and the N-H—O angle is 134.2°). The methoxy phenyl ring is out of plane with the linker segment ( $C8-C9-C1'''-C2''' = 161.4^\circ$ ) as is ring B ( $C3''-C4''-N3-C4 = -66.5^\circ$ ). Ring B has the N-phenyl,N-methyl sulfonamide group attached at the *para* position. The nitrogen of the sulfonamide group is almost perpendicular to ring B ( $N1-S2-C1''-C2'' = 86.2^\circ$ ) forming an “elbow” and the N-phenyl group is almost perpendicular to the long axis of the ligand ( $C1'-N1-S2-C1'' = 70.2^\circ$ ). Finally, ring A is almost perpendicular to the N1-S2 axis ( $C2'-C1'-N1-S2 = 81.2^\circ$ ) and almost forming a parallel aromatic stack with ring B.

The global minimum energy conformer of CID1172084 (**3**) has the midsection of the molecule, that links the rings, in a planar, trans conformation ( $C5'-S1-C2-C3 = -179.8^\circ$ ,  $S1-C2-C3-N4 = -178.4^\circ$ ). The 1,2,4-triazolo[4,3-a]quinoline ring and the thiazole ring are coplanar with the linear section that links them ( $N4'-C5'-S1-C2 = -178.8^\circ$  and  $C3-N4-C1''-N2'' = -179.6^\circ$  respectively). The methoxy group attached on the A ring (carbon C8') of the 1,2,4-triazolo[4,3-a]quinoline ring is nearly in plane with the fused ring system ( $C7'-C8'-O5-C6 = 179.9^\circ$ ) and the *para*-fluoro ring, at the other end of the molecule, is out of plane with the thiazole ring ( $N2''-C3''-C1'''-C2''' = -18.8^\circ$ ).

The global minimum energy conformer of CID2440433 (**4**) has the sulfonamide perpendicular to the phenyl ring ( $C2'-C1'-S3-N2 = -90.0^\circ$ ) and the lone pair of N2 is pointing at the same side as the sulfonamide oxygens ( $C1'-S3-N2-LP = -179.7^\circ$ ). The pyrrolidine is slightly out of plane with the phenyl ring ( $C3'-C4'-N1''-C2'' = 173.7^\circ$ ). The carbonyl group connecting the phenyl ring and the piperazine ring is nearly perpendicular to the phenyl ring pointing on the same side as the methyl groups of the sulfonamide ( $C2'-C3'-C4-O5 = 114.1^\circ$ ). The piperazine N1''' lone pair is pointing on the side of the pyrrolidine and perpendicular to the carbonyl ( $O5-C4-N1'''-LP = 87.4^\circ$ ). The piperazine ring is in a chair conformation and the N4''' lone pair points  $180^\circ$  away from the N1''' lone pair. Finally, the two methyl groups of the dimethylphenyl ring point in the same direction as the N4''' lone pair ( $LP-N4'''-C1''''-C2'''' = 28.0^\circ$ ).

Compound CID1135734 (**5**), 2-[(7-methoxy-4-methyl-[1,2,4]triazolo[4,3-a]quinolin-1-yl)sulfanyl]-*N*-methyl-*N*-(4-phenyl-1,3-thiazol-2-yl)acetamide, an inactive congener of CID1172084 (**3**) was used as a negative control (see Table 1). The global minimum energy conformer of CID1135734 is very similar to the global minimum energy conformer of CID1172084 (**3**). The midsection of the molecule, that links the rings, is in a planar, trans conformation ( $C5'-S1-C2-C3 = -179.3^\circ$ ,  $S1-C2-C3-N4 = 178.2^\circ$ ). The 1,2,4-triazolo[4,3-a]quinoline ring and the thiazole ring are coplanar with the linear section that links them ( $N4'-C5'-S1-C2 = 179.4^\circ$  and  $C3-N4-C1''-N2'' = 178.1^\circ$  respectively). The methoxy group attached on the A ring (carbon C9') of the 1,2,4-triazolo[4,3-a]quinoline ring is nearly in plane with the fused ring system ( $C8'-C9'-O5-C6 = -0.1^\circ$ ) and the phenyl ring, at the other end of the molecule, is out of plane with the thiazole ring ( $N2''-C3''-C1''''-C2'''' = -19.2^\circ$ ).

## Pairwise interaction energies of ligands at the GPR55R\* model.

Tables S-3 through S-6 contain the pairwise interaction energies for the LPI and the CID compounds at the GPR55R\* model.

**Table S-3. Pairwise interaction energies for LPI at GPR55 R\* model.**

Residue	LPI/GPR55 R*		
	Coulomb (kcal/mol)	VdW (kcal/mol)	Total (kcal/mol)
Met1.31	-0.11	-0.25	-0.36
Asn1.50	-0.01	-0.06	-0.07
Phe1.57	0.00	-0.13	-0.13
Leu2.46	0.03	-1.80	-1.78
Ala2.47	0.01	-0.09	-0.08
Asp2.50	0.20	-1.40	-1.20
Leu2.53	0.06	-0.33	-0.28
Lys2.60	-24.81	10.31	-14.50
Met2.61	-0.02	-0.24	-0.26
Gln2.65	-9.45	3.65	-5.80
Glu3.29	3.02	-3.88	-0.86
Tyr3.32	-0.22	-0.88	-1.10
Phe3.33	-0.27	-5.01	-5.28
Met3.36	-0.24	-4.47	-4.71
Tyr3.37	-0.10	-0.58	-0.68
Ser3.39	-0.11	-2.09	-2.20
Val3.40	0.00	-1.95	-1.96
Ile3.43	0.02	-2.28	-2.27
Ile4.60	0.06	-1.25	-1.19
Tyr4.61	-0.10	-3.39	-3.48
Ser4.62	0.16	-0.34	-0.18
Cys168	0.06	-0.36	-0.29
Phe169	-0.37	-3.76	-4.13
His170	-2.25	-2.99	-5.24
Asn171	0.15	-0.59	-0.44
Phe5.39	-0.09	-0.69	-0.78
Phe5.47	0.02	-1.29	-1.27
Ser6.40	0.01	-0.10	-0.09
Val6.43	0.02	-1.48	-1.46
Phe6.44	0.03	-0.98	-0.95
Ser6.47	-0.05	-2.51	-2.56
Phe6.48	0.03	-0.36	-0.34
Pro6.50	0.04	-0.54	-0.50
Val6.51	0.04	-1.56	-1.52
Gln6.58	-2.27	-0.11	-2.38
Val258	-0.12	-0.15	-0.27

Leu7.35	0.02	-4.51	-4.49
Gln7.36	-0.05	-0.52	-0.57
Ser7.38	-0.03	-2.25	-2.28
Met7.39	0.21	-4.35	-4.14
Ser7.42	-0.21	-3.43	-3.64
Asn7.45	-0.03	-2.45	-2.48
Cys7.46	-0.03	-3.42	-3.45
Asp7.49	0.05	-2.27	-2.22
Val7.50	-0.01	-0.39	-0.39
Tyr7.53	0.00	-0.70	-0.69
Water 1	0.02	-0.11	-0.10
Water 2	0.07	-0.86	-0.79
Water 3	0.06	-0.41	-0.35
<hr/>			
LPI			
Conf Expense			6.87
<hr/>			
Grand Total			-89.31
<hr/>			



**Table S-4. Pairwise interactions for CID1792197 (2) at GPR55 R\* model.**

Residue	CID1792197/GPR55 R*		
	Coulomb (kcal/mol)	VdW (kcal/mol)	Total (kcal/mol)
Leu2.53	0.02	-0.16	-0.14
Lys2.60	-5.32	0.76	-4.56
Gln2.65	0.17	-0.44	-0.27
Glu3.29	0.62	-1.30	-0.67
Tyr3.32	0.01	-2.51	-2.49
Phe3.33	-0.27	-4.79	-5.07
Met3.36	-0.20	-5.64	-5.84
Tyr3.37	0.22	-1.66	-1.45
Val3.40	0.03	-3.01	-2.97
Ile3.43	0.03	-0.40	-0.37
Tyr157	0.05	-0.57	-0.52
Phe169	-0.02	-1.39	-1.41
Phe5.39	0.00	-0.20	-0.19
Gly5.46	-0.17	-0.38	-0.55
Phe5.47	-0.16	-3.86	-4.02
Pro5.50	0.03	-0.12	-0.09
Met5.51	0.07	-0.29	-0.22
Met5.54	0.05	-0.06	-0.01
Ser6.39	-0.02	-0.21	-0.23
Val6.43	0.08	-1.62	-1.54
Phe6.44	-0.14	-3.85	-3.98
Val6.45	-0.02	-0.15	-0.16
Ser6.47	-0.20	-3.32	-3.52
Phe6.48	0.02	-0.68	-0.66
Val6.51	0.01	-3.66	-3.65
Gly6.54	0.02	-0.61	-0.59
Phe6.55	-0.09	-2.36	-2.45
Gln6.58	0.06	-1.63	-1.57
Ile266	0.04	-0.19	-0.16
Leu7.35	-0.10	-4.18	-4.28
Gln7.36	-0.17	-0.25	-0.42
Ser7.38	-0.05	-0.45	-0.51
Met7.39	0.12	-2.97	-2.85
Ser7.42	-2.63	1.08	-1.55
Asn7.43	0.03	-0.38	-0.35
Cys7.46	0.01	-1.94	-1.93
Asp7.48	-0.27	-0.36	-0.63
Water	0.03	-0.07	-0.03
CID1792197			
Conf Expense			4.05
Grand Total			-57.84

**Table S-5. Pairwise interactions for CID1172084 (3) at GPR55 R\* model.**

Residue	CID1172084/GPR55 R*		
	Coulomb (kcal/mol)	VdW (kcal/mol)	Total (kcal/mol)
Asp2.50	0.22	-0.23	-0.01
Leu2.53	0.02	-1.56	-1.54
Lys2.60	-4.92	1.60	-3.32
Gln2.65	0.05	-0.22	-0.17
Glu3.29	-0.73	-0.93	-1.66
Tyr3.32	-2.32	-1.13	-3.44
Phe3.33	0.08	-3.57	-3.49
Ser3.35	0.05	-0.22	-0.18
Met3.36	-0.18	-6.03	-6.21
Ser3.39	-0.11	-0.77	-0.87
Val3.40	0.02	-0.66	-0.64
Tyr157	-0.02	-1.30	-1.33
Phe169	-0.10	-1.94	-2.05
His170	0.01	-0.19	-0.18
Asn171	-0.01	-0.15	-0.16
Met172	0.00	-0.43	-0.42
Phe5.39	-0.01	-1.25	-1.26
Phe5.47	0.00	-0.37	-0.37
Val6.43	-0.09	-0.91	-1.00
Phe6.44	-0.02	-0.18	-0.20
Val6.46	0.04	-0.18	-0.14
Ser6.47	-0.91	-1.53	-2.44
Pro6.50	-0.05	-0.42	-0.47
Val6.51	-0.18	-3.07	-3.25
His6.52	-0.01	-0.12	-0.13
Gly6.54	0.13	-1.11	-0.98
Phe6.55	-0.15	-2.42	-2.58
Gln6.58	-0.06	-2.30	-2.36
Phe7.34	0.06	-0.21	-0.15
Leu7.35	0.07	-5.73	-5.65
Ser7.38	-3.83	-0.50	-4.33
Met7.39	0.28	-4.44	-4.16
Phe7.41	-0.12	-3.29	-3.41
Ser7.42	0.01	-4.13	-4.12
Asn7.45	-0.11	-2.83	-2.95
Water	-1.08	0.73	-0.35
CID1172084			
Conf Expense			0.78
Grand Total			-65.19

**Table S-6. Pairwise interaction energies for CID2440433 (4) at GPR55 R\* model.**

Residue	CID2440433/GPR55 R*		
	Coulomb (kcal/mol)	VdW (kcal/mol)	Total (kcal/mol)
Met1.31	0.08	-0.85	-0.77
Lys2.60	-5.12	-0.08	-5.20
Gln2.65	0.70	-3.62	-2.92
Glu3.29	-0.05	-1.24	-1.29
Tyr3.32	-0.02	-0.39	-0.41
Phe3.33	-0.05	-4.27	-4.31
Met3.36	0.15	-1.80	-1.65
Tyr3.37	-0.14	-1.43	-1.57
Val3.40	0.02	-0.07	-0.05
Ile4.60	-0.03	-0.46	-0.49
Tyr157	-0.09	-2.76	-2.84
Phe169	-0.01	-3.80	-3.81
His170	-0.13	-1.04	-1.16
Asn171	-0.02	-1.03	-1.05
Met172	-0.07	-1.07	-1.14
Phe5.39	0.01	-1.40	-1.39
Leu5.42	0.02	-0.67	-0.66
Gly5.46	-0.01	-0.15	-0.16
Phe5.47	-0.10	-1.93	-2.03
Ser6.47	0.02	-0.23	-0.21
Pro6.50	-0.01	-0.18	-0.20
Val6.51	-0.03	-4.38	-4.41
Gly6.54	0.09	-0.41	-0.32
Phe6.55	0.12	-3.61	-3.49
Gln6.58	-1.96	-2.77	-4.73
Val258	0.04	-0.13	-0.09
Ile266	0.00	-0.24	-0.24
Ser7.31	-0.02	-0.26	-0.28
Leu7.35	0.07	-4.59	-4.52
Ser7.38	-0.03	-0.52	-0.55
Met7.39	0.00	-0.96	-0.96
Ser7.42	-0.05	-0.40	-0.46
CID2440433			
Conf Expense			0.46
Grand Total			-52.88

## Other GPR55 Agonists

**Table S-7. Pairwise interaction energies for AM251 at GPR55 R\* model.**

Residue	AM251/GPR55 R*		
	Coulomb (kcal/mol)	VdW (kcal/mol)	Total (kcal/mol)
M1.31	0.00	-0.12	-0.12
K2.60	-5.11	0.29	-4.82
Q2.65	0.26	-2.74	-2.48
E3.29	-0.21	-1.18	-1.39
Y3.32	-0.02	-0.93	-0.95
F3.33	0.12	-4.65	-4.53
M3.36	-0.09	-2.75	-2.84
Y3.37	-0.11	-0.62	-0.72
Y4.61	-0.71	-0.43	-1.14
C168	0.01	-0.31	-0.30
F169	0.01	-2.86	-2.84
H170	0.00	-0.13	-0.13
M172	-0.02	-0.13	-0.15
F5.39	-0.01	-1.63	-1.64
L5.42	0.00	-0.18	-0.18
E5.43	0.18	-0.57	-0.39
F5.47	0.05	-1.62	-1.58
S6.47	0.02	-1.62	-1.60
P6.50	-0.10	-0.98	-1.08
V6.51	-0.12	-5.66	-5.78
H6.52	-0.02	-0.35	-0.37
G6.54	0.31	-1.18	-0.87
F6.55	-0.16	-1.80	-1.96
Q6.58	0.09	-3.23	-3.14
S7.32	-0.01	-0.08	-0.09
F7.34	-0.01	-0.25	-0.25
L7.35	-0.05	-4.83	-4.87
S7.38	-0.27	-2.03	-2.30
M7.39	0.10	-3.34	-3.24
F7.41	0.08	-0.79	-0.71
S7.42	0.14	-2.43	-2.29
AM251			
Conf Expense			-1.13
Grand Total			-53.64

AM251 is a smaller molecule than the CID compounds but similar in overall length and width to CID2440433, the shortest of the four. Unlike the CID compounds that have most of their bulk in the loop region, AM251 fits in the binding site with most of its bulk in the transmembrane region

and only its piperidine ring in the loop area. It reaches as deeply in the receptor TMH region and as high in the extracellular loop region as CID2440433. However, its bulk is closer to TMHs 6 and 7 compared to CID2440433 that is closer to TMHs 5 and 6.

The binding site of AM251 is between TMHs 2, 3, 6, and 7. AM251 forms fewer hydrogen bonds and aromatic stacks than the larger LPI and the CID compounds but has a number of hydrophobic interactions with the residues of the binding site. Similar to the CID compounds, the primary interaction for AM251 is between its carboxamide oxygen and K2.60(80). The hydrogen bond (N-O) distance is 2.59Å and the (N-H—O) angle is 176°. Also, its pyrazole ring forms an aromatic stack with F3.33(102) with a ring centroid to centroid distance of 4.75Å and an angle of 73°. The total interaction energy for AM251 with GPR55 is -56.38 kcal/mol (see Table S-7 above). The major contributions are the Van der Waals interactions with V6.51(242) and L7.35(270) followed by the aromatic stacking interaction with F3.33(102) and the hydrogen bonding interaction with K2.60(80). Van der Waals interactions with M3.36(105), Q6.58(249), S7.38(273) and M7.39(274) add also to the overall interaction energy to a lesser extent. See image below, EC3 and TMH7 have been omitted for clarity.

**Figure S-2.** AM251 docked in the GPR55R\* model is illustrated here. The view is from lipid with the EC3 loop and TMH7 omitted for clarity.

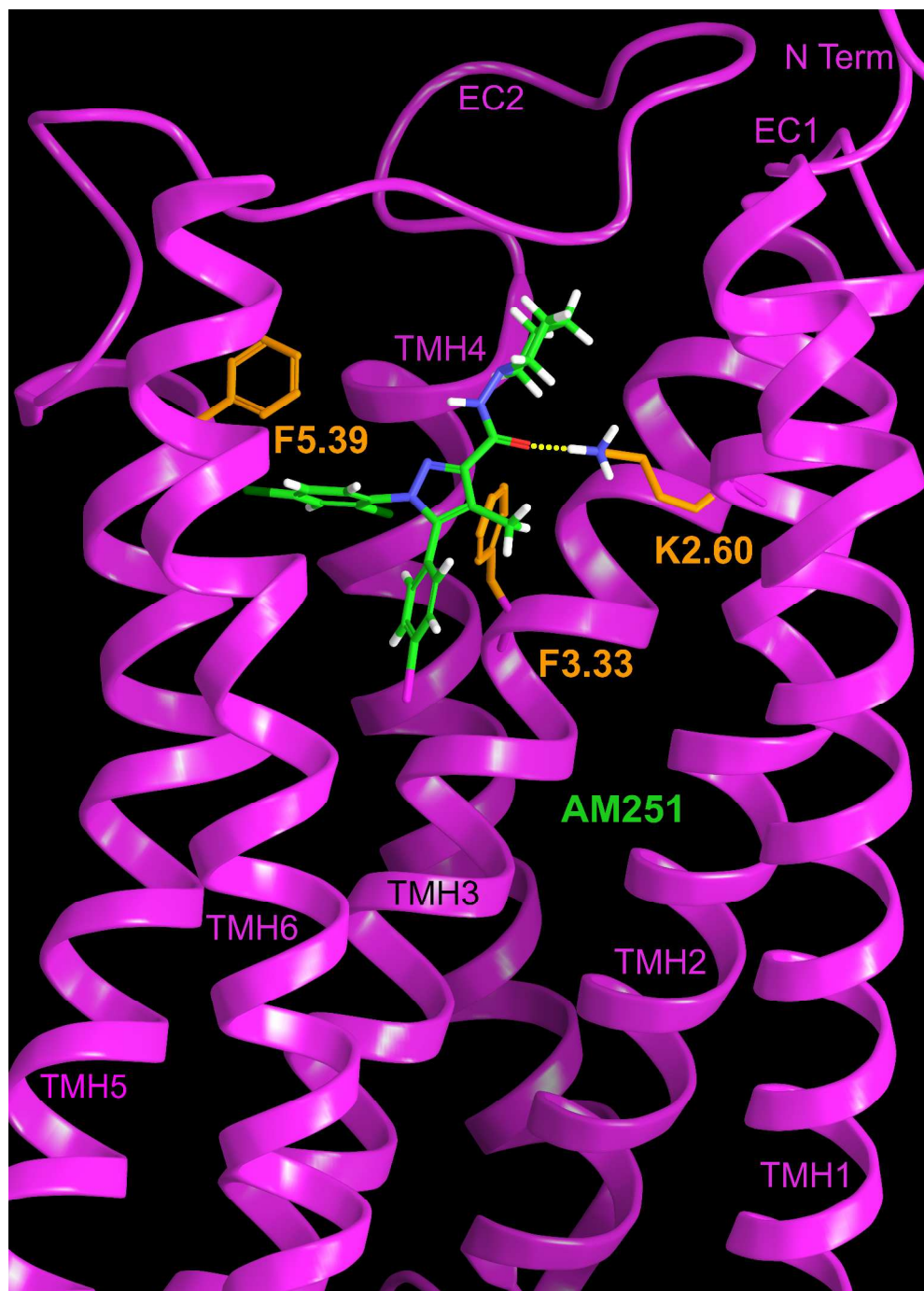


**Table S-8. Pairwise interaction energies for GSK494581A at GPR55 R\* model.**

Residue	GSK494581A/GPR55 R*		
	Coulomb (kcal/mol)	VdW (kcal/mol)	Total (kcal/mol)
L2.53	0.01	-0.04	-0.03
K2.60	-5.11	-0.61	-5.72
Q2.65	0.39	-1.70	-1.31
E3.29	-0.57	-2.98	-3.55
Y3.32	-0.05	-0.80	-0.85
F3.33	-0.05	-5.73	-5.79
M3.36	0.07	-1.36	-1.28
Y3.37	-0.20	-0.91	-1.11
I4.60	-0.39	-0.85	-1.24
Y4.61	-1.84	-2.10	-3.94
S4.62	-0.13	-0.34	-0.47
H160	-0.70	-0.98	-1.68
C168	-0.02	-0.29	-0.32
F169	-0.09	-2.58	-2.67
H170	0.07	-4.49	-4.42
N171	-0.15	-1.36	-1.51
M172	-0.08	-0.73	-0.81
S173	-0.02	-0.05	-0.07
T176	0.01	-0.13	-0.12
W177	0.02	-0.11	-0.09
V5.38	-0.05	-1.26	-1.30
F5.39	-0.08	-2.66	-2.74
L5.42	-0.07	-0.75	-0.81
F5.47	0.05	-1.55	-1.50
S6.47	0.00	-1.24	-1.23
F6.48	0.00	-0.24	-0.24
P6.50	-0.06	-0.53	-0.58
V6.51	-0.03	-3.54	-3.57
G6.54	0.04	-0.17	-0.13
Q6.58	-2.45	-0.31	-2.76
F256	-0.03	-0.20	-0.23
L7.35	0.04	-1.96	-1.92
S7.38	0.30	-1.60	-1.30
M7.39	0.14	-0.93	-0.79
C7.40	-0.01	-0.07	-0.08
S7.42	-0.03	-0.93	-0.96
GSK494581A			
Conf Expense			4.39
Grand Total			-52.74

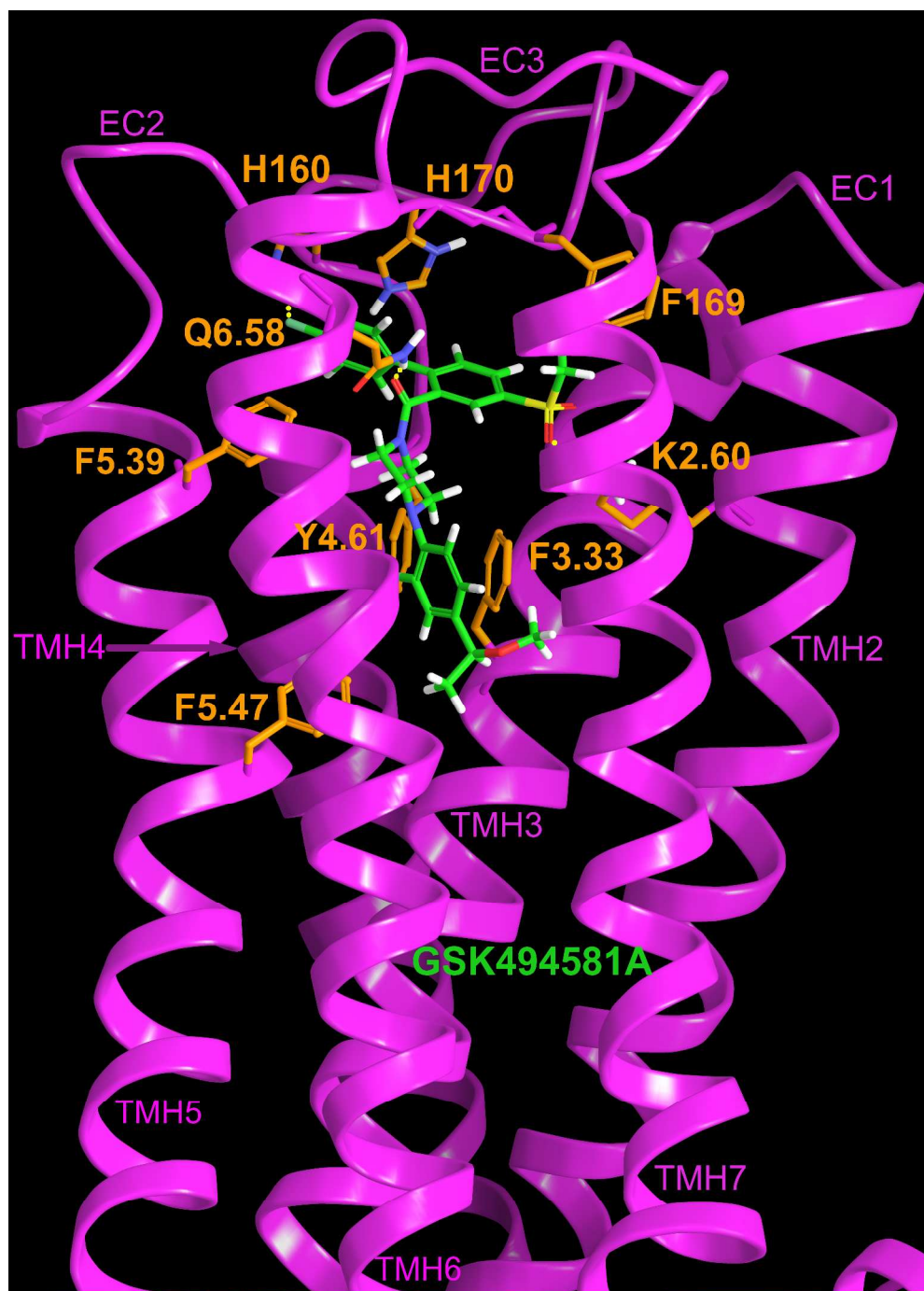
The best compound mentioned in the Brown et. al. paper (1), GSK494581A, is very similar to the CID2440433 compound we discuss in the paper. They have the same general shape (T) and only the substituents change (phenyl instead of pyrrolidine and methyl sulphonyl instead of dimethyl sulphonamide of the central phenyl ring, and methylmethoxy toluene instead of 2,3-dimethyl benzene of the piperazine ring). The compound was built and docked in the GPR55 R\* model and it occupies the same area as the closely related CID2440433 compound. The vertical part of the T is located between the transmembrane helices and the cross bar of the T is in the horizontal region of the binding pocket which is an area underneath the extracellular loops just like compound CID2440433. See Figure S-3.

The GSK494581A sulfonamide oxygen forms a hydrogen bond with K2.60(80) and Q6.58(249) hydrogen bonds with the carbonyl oxygen above the piperazine ring. The hydrogen bond (N-O) and (N-O) distances and (N-H—O) and (N-H—O) angles are 2.77Å and 2.74Å and 163° and 168° respectively. The GSK494581A 4-fluorophenyl ring hydrogen bonds with H160 and 2-fluorophenyl ring has a hydrogen bond with Y4.61. The hydrogen bond (N-F) and (O-F) distances and (N-H—F) and (O-H—F) angles are 2.97Å and 2.52Å and 130° and 167° respectively. GSK494581A also forms a number of  $\pi$ - $\pi$  stacking interactions with the receptor. The benzene ring adjacent to the sulfonamide forms aromatic T-stacks with F169 and H170 of the EC-2 loop (ring centroid to ring centroid distances 6.60Å and 5.86Å respectively and angles between ring planes 28° and 80° respectively). The 4-chlorophenyl ring forms two aromatic stacks: one with H170 and one with F5.39(182). The ring centroid to ring centroid distances are 4.14Å and 6.32Å respectively and angles between ring planes 42° and 83° respectively. The 2-fluorophenyl ring adjacent to the piperazine forms aromatic stack with the residues F3.33(102)



and F5.47(190) (ring centroid to ring centroid distances 6.92Å and 6.25Å respectively and angles between ring planes 29° and 56° respectively). The total interaction energy for GSK494581A at this docking site in GPR55 is -52.74 kcal/mol (see Table S-8). The hydrogen bonding interaction with K2.60(80) and the stacking interaction with F3.33(102) are major contributors to the interaction energy, as well as the aromatic stacking interactions with H170 and the hydrogen bonding interaction with Y4.61. However, the Van der Waals interactions with the hydrophobic residues E3.29(98) and V6.51(242) (residues not shown in Figure S-3) make a substantial contribution to the overall interaction energy.

**Figure S-3.** GSK494581A docked in the GPR55R\* model is illustrated here. The view is from lipid between TMH6 and 7. TMH1 has been omitted here for clarity.



## Literature Cited

1. Brown, A. J., Daniels, D. A., Kassim, M., Brown, S., Haslam, C. P., Terrell, V. R., Brown, J., Nichols, P. L., Staton, P. C., Wise, A., and Dowell, S. J. (2011) Pharmacology of GPR55 in Yeast and Identification of GSK494581A as a Mixed-Activity Glycine Transporter Subtype 1 Inhibitor and GPR55 Agonist, *J Pharmacol Exp Ther* 337, 236-246.